

Optical study of the charge-density-wave mechanism in $2H$ -TaS₂ and Na_xTaS₂

W. Z. Hu,¹ G. Li,¹ J. Yan,¹ H. H. Wen,¹ G. Wu,² X. H. Chen,² and N. L. Wang^{1,*}

¹*Beijing National Laboratory for Condensed Matter Physics, Institute of Physics, Chinese Academy of Sciences, Beijing 100080, P. R. China*

²*Hefei National Laboratory for Physical Science at Microscale and Department of Physics, University of Science and Technology of China, Hefei 230026, P. R. China*

We report an optical study of transition metal dichalcogenide $2H$ -TaS₂ and Na intercalated superconductor Na_xTaS₂ over a broad frequency range at various temperatures. A clear gap feature was observed for $2H$ -TaS₂ when it undergoes a CDW transition. The existence of a Drude component in $\sigma_1(\omega)$ below T_{CDW} indicates that the Fermi surface of $2H$ -TaS₂ is only partially gapped in CDW state. The spectral evolution of two different Na_xTaS₂ crystals further confirms that the partial gap structure observed in $2H$ -TaS₂ has a CDW origin. The CDW mechanism for $2H$ -TaS₂, the competition between CDW and superconductivity in Na_xTaS₂ system are discussed.

PACS numbers: 78.20.-e, 71.45.Lr

Charge density wave (CDW) order and its coexistence with superconductivity in $2H$ type transition metal dichalcogenides (TMDC) has been one of the major subjects in condensed matter physics since 1970's. The name " $2H$ " is derived from structural character where " 2 " represents two chalcogen-metal-chalcogen sandwiches in one unit cell and " H " stands for "hexagonal". In this family, $2H$ -TaSe₂ has an incommensurate followed by a commensurate CDW transitions at 122K and 90K; while $2H$ -TaS₂ and $2H$ -NbSe₂ only undergo one incommensurate CDW transition at 75K and 35K, respectively¹. On the contrary, the superconducting transition temperature T_c increases from $2H$ -TaSe₂ over $2H$ -TaS₂ to $2H$ -NbSe₂, suggesting that the CDW order and superconductivity compete. Additionally, upon intercalation of Na into $2H$ -TaS₂, T_{CDW} is suppressed but T_c increases from 0.8 to 4.4 K, yielding further evidence for the competition between these two orders². Although it is generally believed that the superconductivity in $2H$ -TMDC is caused by conventional electron-phonon coupling, the driving mechanism for CDW transition is still not well understood. Different viewpoints including Fermi surface (FS) nesting³, saddle point mechanism⁴ or other hidden order in \mathbf{k} space^{5,6} have been proposed to explain the CDW instability, but no consensus has been reached.

Optical spectroscopy is a powerful bulk sensitive technique with high energy resolution, but previous researches on the in-plane optical properties of $2H$ -TaSe₂ and $2H$ -NbSe₂ did not find any sharp changes directly related to CDW transition⁷. As $2H$ -TaS₂ has only one CDW transition with relatively higher T_{CDW} , it is therefore an ideal system to study CDW mechanism in $2H$ -TMDC family. However, no detailed optical research was performed on $2H$ -TaS₂ except some early work on the high energy structure at room or liquid N₂ temperatures⁸. In this work, we report the first detailed optical study of $2H$ -TaS₂ and Na_xTaS₂ over a broad frequency range at various temperatures to reveal the CDW mechanism. The overall frequency dependent reflectivity $R(\omega)$ of $2H$ -TaS₂ shows a metallic response, but a mid-infrared suppression feature emerges below T_{CDW} . The

real part of conductivity $\sigma_1(\omega)$ is composed of a Drude response together with a weak mid-infrared peak in the CDW state, indicating a partial gap was formed on the Fermi surface. For Na_xTaS₂, CDW features turn weaker and tend to disappear as Na content increases. All those optical results, being consistent with the transport measurements obtained on the same crystals, can be well understood in the frame of FS nesting mechanism.

$2H$ -TaS₂ single crystals were grown by chemical iodine-vapor transport method. High purity Ta (99.95%) and S (99.5%) powder were mixed, thoroughly ground, pressed into a pellet, and sealed under vacuum in a quartz tube ($\varnothing 13$ mm \times 150 mm) with iodine (10 mg/cm⁻³). Single crystals were obtained after growing at 720-700°C for a week and cooling down slowly to room temperature. $2H$ type Na_xTaS₂ single crystals were grown by chemical reaction, as described previously². The T-dependent resistivity was obtained by four contacts technique in a Quantum Design PPMS and the results are shown in Fig. 1. There is a clear CDW transition at 75K for $2H$ -TaS₂, while such feature is vague around 65K for Na_xTaS₂ $T_c=2$ K sample, and totally disappears in the higher Na content crystals ($T_c=4.2$ K). The supercon-

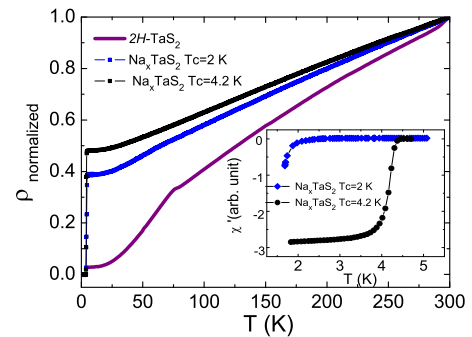


FIG. 1: (color online) T-dependent resistivity for $2H$ -TaS₂ and two Na_xTaS₂ crystals (all normalized to values at 300 K). The inset shows the real part of ac susceptibility below 5K, which identifies T_c for two Na_xTaS₂ crystals 2 K and 4.2 K, respectively.

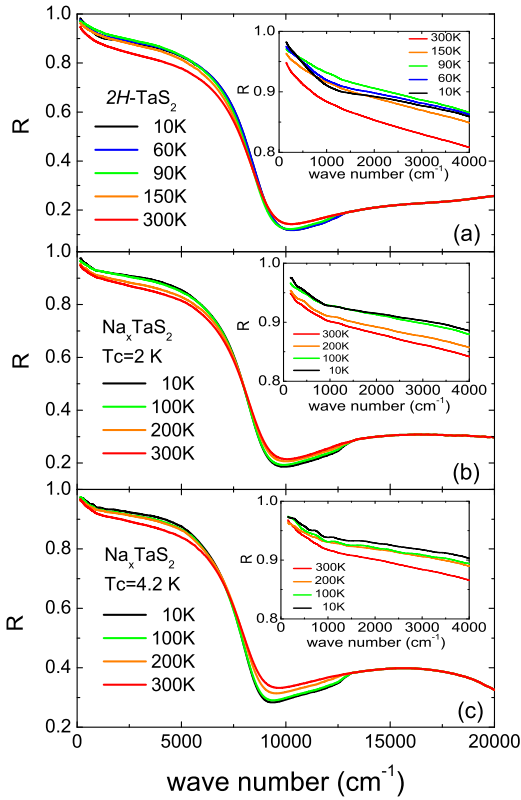


FIG. 2: (color online) Reflectivity of (a) $2H\text{-TaS}_2$ (b) Na_xTaS_2 ($T_c=2$ K) (c) Na_xTaS_2 ($T_c=4.2$ K) from 150 cm^{-1} to 20000 cm^{-1} at various temperatures. The inset figures focus on the spectra from 150 cm^{-1} to 4000 cm^{-1} .

ducting transition temperature for Na_xTaS_2 was identified by ac susceptibility as shown in the inset.

Optical experiments were carried out on as-grown surfaces by a Bruker IFS 66v/s spectrometer in the range from 30 to $25,000$ cm^{-1} with *in-situ* overcoating technique to get the in-plane reflectivity. Considering the small size of our samples (about 1.5×2 mm^2), data below 150 cm^{-1} are cut off for reliability. Fig. 2 shows the T-dependent $R(\omega)$ for $2H\text{-TaS}_2$ and Na_xTaS_2 , both display a metallic behavior, including the high reflectance at low ω , a sharp drop in the near-infrared region (plasma edge), and interband transitions at higher frequencies. The difference between the pure and intercalated materials in low energies is evident. For $2H\text{-TaS}_2$, $R(\omega)$ at 10 K and 60 K are suppressed below the curve of 90 K from 400 to 5000 cm^{-1} . This is a typical partial-gap behavior on Fermi surface manifested in reflectance⁹. Similar suppression is weak in Na_xTaS_2 $T_c=2$ K sample, and almost invisible in $T_c=4.2$ K sample with higher Na content.

Fig. 3 illustrates the real part of conductivity obtained by Kramers-Kronig transformation of $R(\omega)$ at selected temperatures. The inset shows $\sigma_1(\omega)$ below 4000 cm^{-1} at 10 K. The existence of the Drude component at all temperatures in both $2H\text{-TaS}_2$ and Na_xTaS_2 confirms their metallic behavior. For $2H\text{-TaS}_2$, a mid-infrared peak emerges below T_{CDW} and vanishes at higher T. In or-

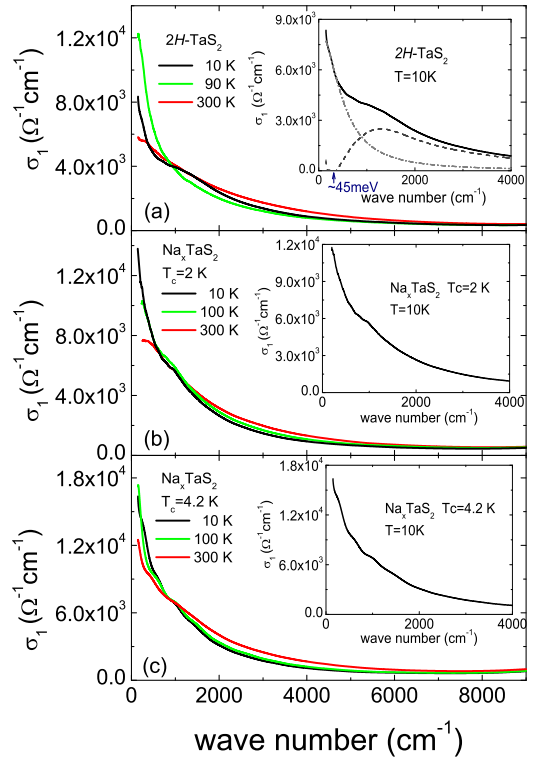


FIG. 3: (color online) The real part of conductivity of (a) $2H\text{-TaS}_2$ (b) Na_xTaS_2 ($T_c=2$ K) (c) Na_xTaS_2 ($T_c=4.2$ K) from 150 cm^{-1} to 9000 cm^{-1} at selected temperatures. The inset figures amplified the spectra at 10 K from 150 cm^{-1} to 4000 cm^{-1} . For $2H\text{-TaS}_2$, the experiment result, a Drude fit, and $\sigma_1(\omega)$ subtracts Drude fit is plotted by black line, gray dash dot line, dark gray dash line, respectively.

der to clarify this feature, we use Drude model to fit the low frequency part of 10 K's curve and subtract this free-carrier contribution from the experiment result, as shown in inset of Fig. 3 (a). Then we get a gap of 45 meV , close to reported CDW-gap value of 50 meV by STM experiment¹⁰. As the scattering rate $1/\tau$ in simple Drude model is a frequency independent constant, such fitting is just a qualitative analysis. In Na_xTaS_2 case, similar gap-like feature is obscure and shifts to lower energy for Na_xTaS_2 $T_c=2$ K sample, and almost disappears in the higher Na content crystal. Since the mid-infrared peak in $\sigma_1(\omega)$ appears only below T_{CDW} for CDW-bearing samples, and vanishes in Na_xTaS_2 with no CDW transition, which consist with dc transport results, thus this peak in $\sigma_1(\omega)$ has a CDW origin. As the Drude response coexists with the mid-infrared peak below T_{CDW} , the Fermi surface is only partially gapped in the CDW state.

It is well known that a partial gap structure can be well resolved in the spectrum of the frequency dependent scattering rate $\Gamma(\omega)$ ^{9,11}. Fig. 4 shows the $\Gamma(\omega)$ spectra for those samples obtained from the extended Drude model $\Gamma(\omega)=(\omega_p^2/4\pi)\text{Re}[1/(\sigma(\omega))]$, where ω_p is the overall plasma frequency and can be obtained by summarizing $\sigma_1(\omega)$ up to the reflectance edge frequency. The

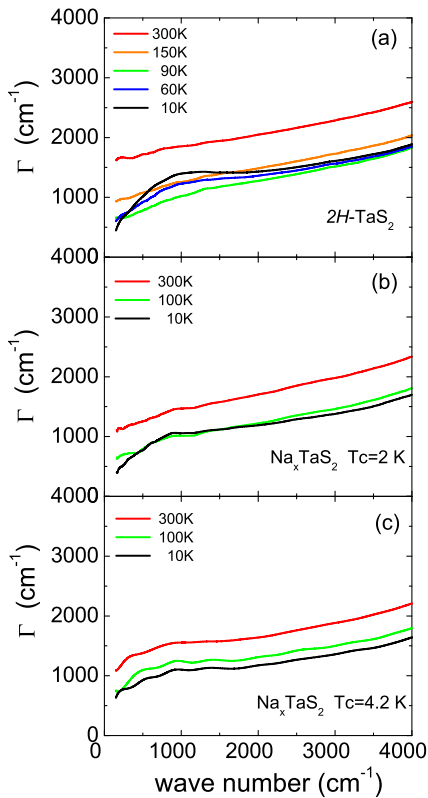


FIG. 4: (color online) The scattering rate of (a) $2H$ -TaS₂ (b) Na_xTaS₂ ($T_c=2$ K) (c) Na_xTaS₂ ($T_c=4.2$ K)

obtained ω_p values are roughly 2.4×10^4 cm⁻¹ for $2H$ -TaS₂, 2.6×10^4 cm⁻¹ for Na_xTaS₂ $T_c=2$ K sample and 3.0×10^4 cm⁻¹ for Na_xTaS₂ $T_c=4.2$ K sample, respectively. For $2H$ -TaS₂, above T_{CDW} , $\Gamma(\omega)$ is almost unchanged in shape but decreases in magnitude as T decreases. In the CDW state, a broad peak forms around 1000 cm⁻¹ and gets stronger at 10K. For Na_xTaS₂, similar feature is weak and shifts slightly to lower energy, and tends to vanish eventually at higher Na content. We note that the spectral feature in $\Gamma(\omega)$ is very similar to the behavior in other materials with a partially gapped Fermi surface, such as the antiferromagnet Cr where a spin-density-wave gap opens on parts of the FS¹¹, and the electron-doped high- T_c cuprate Nd_{2-x}Ce_xCuO₄ in which a spin-correlation gap appears at "hot spots" (the intersecting points of the FS with the antiferromagnetic zone boundary)⁹. In comparison with those work, the $\Gamma(\omega)$ spectra shown in Fig. 4 further clarifies the existence of CDW partial gap on the FS in $2H$ -TaS₂ and its vanishing tendency upon Na-intercalation. We emphasize that the CDW gap feature in optics is weak in $2H$ -TaS₂. Early work based on other technique indicated that only 10 to 20% FS were removed by CDW gap in $2H$ -Ta materials³. Qualitatively, our result is consistent with those work.

As shown above, we identified the formation of CDW induced partial gap and its evolution with Na intercalation. Before giving further discussion on charge-density-

wave mechanism, a brief review about ARPES results is necessary. Previous studies on $2H$ -NbSe₂^{12,13,14,15}, $2H$ -TaS₂¹⁴ and $2H$ -TaSe₂^{16,17} showed that they all have similar Fermi surface, i.e., two double-wall hole pockets around Γ and K . Especially, a recent research indicates that Na_xTaS₂ also has such two-pockets Fermi surface⁶. Apart from observations of FS topology, the existence of saddle point at $1/2 \Gamma K$ ¹³, or extended saddle band along ΓK ^{14,16,18} were confirmed by ARPES for $2H$ -TMDC.

The key requirement for any CDW mechanism is the direct observation of a CDW gap, and a match between the nesting vector which links the gapped region and the CDW vector associated with the lattice superstructure. Fermi surface nesting is a traditional mechanism for CDW transitions, which predicts the opening of charge-density-wave gap at parallel regions of Fermi surface connected by CDW vector. For $2H$ -TMDC members, the possibility about Γ pocket self nesting at parallel hexagon boundaries¹³ has been excluded because the distance between two nesting regions does not match the length of CDW vector associated with the nearly 3×3 superlattice, and no CDW gap was found around Γ pocket^{6,14,15,16,17,18,19}. On the other hand, there are evidences for a weak nesting at Fermi surface around K ^{3,15,17,20}, and the energy gap around inner K pocket below T_{CDW} was clearly observed in $2H$ -TaSe₂^{16,17} and $2H$ -TaS₂¹⁴. Besides FS nesting scenario, saddle point mechanism is another traditional model which regards the saddle points close to E_F as scattering "sink" and their removal in the CDW state will enhance dc conductivity⁴. But saddle point's position observed by ARPES would lead to a 2×2 superlattice, inconsistent with the nearly 3×3 superlattice for $2H$ -TMDC in the CDW state. Moreover, the saddle band is not so close to the Fermi energy^{13,14,15} as Rice and Scott predicted. Therefore, some recent ARPES studies try to find other "hidden" order in \mathbf{k} space to explain the CDW instability, such as the CDW-vector-matched saddle points where the "gap" follows BCS description in CDW state⁵ or special "gapped" regions around M point of the Brillouin zone⁶. In fact, M is close to K pocket, and "gap" appears around M is usually accompanied by the opening of a real CDW gap on FS around K pocket. Specially, for energy band which does not across E_F , the observation of band dispersion anomaly is not a real "gap" but an "energy shift"^{16,18}, so "gapped" region around M point cannot account for charge-density-wave instability in $2H$ -TMDC.

Optical probe offers supplementary information on charge excitations with high energy resolution, and its result should be consistent with ARPES observation. On this basis, our data can be naturally understood in the frame of Fermi surface nesting mechanism. First of all, we observe the temperature evolution of a partial gap formed on Fermi surface, which is directly related to the onset of charge-density-wave transition. For $2H$ -TaS₂, both the suppression in $R(\omega)$, the mid infrared peak in $\sigma_1(\omega)$, and the broad peak in $\Gamma(\omega)$ below T_{CDW} testify

the existence of a gapped Fermi surface in CDW state. In addition, all those special characters turn weaker after Na intercalation, and tend to disappear with increasing Na content, which again convince that these characters have a CDW origin. As the Drude component in $\sigma_1(\omega)$ never disappears at all temperatures, the free carrier contribution exists in the CDW state, consistent with the fact that Γ pocket is unaffected in the CDW state for both $2H$ -TaS₂¹⁴ and low Na content Na_xTaS₂⁶. ARPES experiments indicate that the Γ pocket dominates the transport properties¹⁹, formation of a CDW gap at K pocket, which plays a less role in transport above T_{CDW} , would reduce the scattering channels, therefore enhance the metallic behavior in CDW state, thus the resistivity drops after CDW transition for $2H$ -TaS₂ and Na_xTaS₂ $T_c=2$ K samples. The FS nesting mechanism can also help in understanding why Na intercalation suppresses CDW transition and increases T_c . As evidenced by ARPES experiments, both the inner and outer K pockets contribute to superconductivity by opening up superconducting gaps below T_c in those region which were not gapped by CDW ordering^{21,22}. Here we should keep in mind that only certain regions of inner K pocket satisfy the CDW nesting condition^{3,15,17,20}. With Na intercalation, the shapes of Fermi surfaces surrounding both Γ and K are expected to change. This was confirmed by recent ARPES research on Na_xTaS₂ crystals⁶. Then it is

possible that some regions of K pocket would no longer be nested upon Na intercalations, leading to a gradual reduction of gapped region at Fermi surface, therefore the CDW gap feature in $\sigma_1(\omega)$ and $\Gamma(\omega)$ for Na_xTaS₂ crystals are weaker than that of $2H$ -TaS₂. As fewer region at the K pocket can be gapped in the CDW state, density of states at Fermi energy would be larger than the case in $2H$ -TaS₂, following BCS theory, T_c will increase as a result.

In conclusion, we report the optical study of $2H$ -TaS₂ and Na_xTaS₂ over a broad frequency range at various temperatures. Both the mid-infrared suppression in $R(\omega)$, the peak in $\sigma_1(\omega)$ and $\Gamma(\omega)$ appear in accord with the onset of CDW transition, signaling the formation of a partial gap on Fermi surface in the CDW state. The gradual removal of CDW character for two different Na_xTaS₂ samples further confirm the gap-like features observed in $2H$ -TaS₂ have a CDW origin. The charge-density-wave mechanism in $2H$ -TMDC and Na's role in the suppression of CDW can be understood in the frame of Fermi surface nesting mechanism. Specifically, we suggest the K pocket is not only responsible for CDW instability, but also contributes largely to superconductivity.

This work is supported by National Science Foundation of China, the Knowledge Innovation Project of Chinese Academy of Sciences, and the 973 project of Ministry of Science and Technology of China.

-
- * Electronic address: nlwang@aphy.iphy.ac.cn
- ¹ J. A. Wilson and A. D. Yoffe, Adv. Phys. **18**, 193 (1969); J. A. Wilson, F. J. Di Salvo and S. Mahajan, Adv. Phys. **24**, 117 (1975); D. E. Moncton, J. D. Axe, and F. J. DiSalvo, Phys. Rev. B **16**, 801 (1977).
 - ² L. Fang, Y. Wang, P. Y. Zou, L. Tang, Z. Xu, H. Chen, C. Dong, L. Shan, and H. H. Wen, Phys. Rev. B **72**, 014534 (2005).
 - ³ J. A. Wilson, Phys. Rev. B **15**, 5748 (1977).
 - ⁴ T. M. Rice and G. K. Scott, Phys. Rev. Lett. **35**, 120 (1975).
 - ⁵ O. Seifarth, S. Gliemann, M. Skibowski, L. Kipp, Journal of Electron Spectroscopy and Related Phenomena **137-140**, 675 (2004).
 - ⁶ D. W. Shen, B. P. Xie, J. F. Zhao, L. X. Yang, L. Fang, J. Shi, R. H. He, D. H. Lu, H. H. Wen, and D. L. Feng, cond-mat/0612064.
 - ⁷ A. S. Barker, Jr., J. A. Ditzemberger, and F. J. Di Salvo, Phys. Rev. B **12**, 2049 (1975); V. Vescoli, L. Degiorgi H. Berger and L. Forr, Phys. Rev. Lett. **81**, 453 (1998); S. V. Dordevic, D. N. Basov, R. C. Dynes, and E. Bucher, Phys. Rev. B **64**, 161103(R) (2001); S. V. Dordevic, D. N. Basov, R. C. Dynes, B. Ruzicka, V. Vescoli, L. Degiorgi, H. Berger, R. Gal, L. Forr, and E. Bucher, Eur. Phys. J. B **33**, 15 (2003).
 - ⁸ A. R. Beal, H. P. Hughes and W. Y. Liang J. Phys. C: Solid State Phys. **8**, 4236 (1975); S. S. P. Pakkin and A. R. Beal, Philo. Mag. B **42**, 627 (1980).
 - ⁹ N. L. Wang, G. Li, Dong Wu, X. H. Chen, C. H. Wang, and H. Ding, Phys. Rev. B **73**, 184502 (2006).
 - ¹⁰ C. Wang, B. Giambattista, C. G. Slough, and R. V. Coleman, Phys. Rev. B **42**, 8890 (1990).
 - ¹¹ D. N. Basov, E. J. Singley, and S. V. Dordevic, Phys. Rev. B **65**, 054516 (2002).
 - ¹² T. Kiss, T. Yokoya, A. Chainani, S. Shin, M. Nohara, H. Takagi, Physica B **312-313**, 666 (2002)
 - ¹³ Th. Straub, Th. Finteis, R. Claessen, P. Steiner, S. Hfner, P. Blaha, C. S. Oglesby, and E. Bucher, Phys. Rev. Lett. **82**, 4504 (1999).
 - ¹⁴ W. C. Tonjes, V. A. Greanya, R. Liu, C. G. Olson, and P. Molinie, Phys. Rev. B **63**, 235101 (2001).
 - ¹⁵ K. Rossnagel, O. Seifarth, L. Kipp, M. Skibowski, D. Voß, P. Kruger, A. Mazur, and J. Pollmann, Phys. Rev. B **64**, 235119 (2001).
 - ¹⁶ R. Liu, W. C. Tonjes, V. A. Greanya, C. G. Olson, and R. F. Frindt, Phys. Rev. B **61**, 52125762 (2000).
 - ¹⁷ K. Rossnagel, Eli Rotenberg, H. Koh, N. V. Smith, and L. Kipp, Phys. Rev. B **72**, 121103(R) (2005).
 - ¹⁸ R. Liu, C. G. Olson, W. C. Tonjes, and R. F. Frindt, Phys. Rev. Lett. **80**, 5762 (1998).
 - ¹⁹ T. Valla, A.V. Fedorov, P. D. Johnson, J. Xue, K. E. Smith, and F. J. DiSalvo, Phys. Rev. Lett. **85**, 4759 (2000).
 - ²⁰ G. Wexler and A. M. Woolley, J. Phys. C: Solid State Phys. **9**, 1185 (1976).
 - ²¹ T. Valla, A.V. Fedorov, P. D. Johnson, P-A. Glans, C. McGuinness, K. E. Smith, E.Y. Andrei, H. Berger, Phys. Rev. Lett. **92**, 086401 (2004).
 - ²² T. Yokoya, T. Kiss, A. Chainani, S. Shin, M. Nohara, H. Takagi, Science **294**, 2518 (2001).